Eur. Phys. J. B **8**, 363–369 (1999)

THE EUROPEAN PHYSICAL JOURNAL B

EDP Sciences

Low temperature Kondo reduction of quadrupolar and magnetic moments in the $YbCu_{5-x}Al_x$ series

P. Bonville[1,a], E. Vincent[1], and E. Bauer[2]

[1] CEA, Centre d'Études de Saclay, DSM/Service de Physique de l'État Condensé, 91191 Gif-sur-Yvette, France
[2] Institut für Experimental Physik, Technische Universität Wien, 1040 Wien, Austria

Received 16 April 1998

Abstract. We present measurements in the $YbCu_{5-x}Al_x$ series, down to the 50 mK range, using ^{170}Yb Mössbauer absorption spectroscopy and magnetisation measurements. In this series, the hybridisation between the Yb $4f$ electrons and the conduction electrons is known to decrease as the Al content x increases. We apply the variational solution of the impurity Kondo problem to the interpretation of our data. We show that the Kondo temperature can be derived from the measured $4f$ quadrupole moment and, for the magnetically ordered compounds ($x \geq 1.6$), we obtain the exchange energy as a function of the Al content. Our findings are in general agreement with Doniach's model describing the onset of magnetic ordering according to the relative values of the Kondo and exchange energy scales.

PACS. 71.27.+a Strongly correlated electron systems; heavy fermions – 75.30.Mb Valence fluctuation, Kondo lattice, and heavy-fermion phenomena – 76.80.+y Mössbauer effect; other γ-ray spectroscopy

1 Introduction

In previous works ([1] and references therein), it was shown that a progressive substitution of Al for Cu in $YbCu_5$ leads to a decrease of the hybridisation between the Yb $4f$ electrons and the metal electrons: the Yb ion has an intermediate valence in $YbCu_5$ whereas it is nearly trivalent in $YbCu_3Al_2$. Above a critical Al content $x_c \simeq 1.5$, the state with magnetic ordering of the Yb ions becomes the more stable. Concomitantly, the specific heat data for compounds around this critical concentration reveal the occurrence of a Non-Fermi liquid behaviour ($1.3 \leq x \leq 1.6$). The valence v of the Yb ion, for $x \geq 1.3$, has been determined by L_{III}-edge X-ray absorption to be 2.98, *i.e.* the number of holes in the $4f$ shell is 0.98. The $YbCu_{5-x}Al_x$ compounds for $x \geq 1.3$ are therefore Kondo lattices where the magnetic properties as well as the characteristic energy scales (Kondo coupling, exchange interaction) are expected to vary smoothly with the Al concentration. Among the various theories dealing with a Kondo impurity or a lattice of Kondo ions [2], the variational approach to the impurity Kondo problem introduced by Gunnarsson and Schönhammer [3] allows the calculation of the $T = 0$ properties of a Kondo ion in a rather tractable manner. Although this model cannot be claimed to describe the features of a Kondo lattice in detail, it allows a comparison of measured low temperature electronic observables with theoretical predictions to be made; it is also easily extended to the case of a crystal field degeneracy lifting of the $4f$ shell [4–6], which is of great practical importance for the Ce^{3+} or Yb^{3+} ion in the nearly trivalent (or Kondo) limit.

In the present work, we will be interested in the low temperature properties of the Yb^{3+} ion in the $YbCu_{5-x}Al_x$ series for $x \geq 1.3$, obtained by ^{170}Yb Mössbauer absorption spectroscopy and magnetisation measurements down to temperatures in the 50 mK range. We present Mössbauer data for compounds with $x = 1.3$, 1.4, 1.5, 1.6, 1.7 and 1.75, and magnetic susceptibility data for $x = 1.6$ and 1.7. We will also incorporate in this work the results obtained for $YbCu_3Al_2$ ($x = 2$) [7]. The experimental findings will be interpreted with the help of the variational approach, with the aim of extracting the Kondo and exchange energy scales throughout the series. The use of a single ion model, characterised by a single ion Kondo temperature, to describe the properties of a Kondo lattice (except for the low temperature resistivity where coherence effects between Kondo scattering centers can be important) can be justified as the Kondo coupling is essentially an on-site interaction. In the presence of intersite magnetic interactions, treated in the molecular field approximation, single ion models can be thought to describe rather well the magnetic properties, provided one deals with localised magnetism and not with band magnetism [6].

2 The variational approach to the Kondo impurity problem

The variational solution of the Anderson Hamiltonian describing a paramagnetic ion hybridised with conduction

[a] e-mail: bonville@spec.saclay.cea.fr

electrons [3] is derived by minimizing the energy of the ground N-electron state represented by the trial function:

$$|\psi\rangle = A\left[|\Omega\rangle + \frac{1}{N_f}\sum_{m,k<k_F} a_{km} f_m^\dagger c_{km}|\Omega\rangle\right]. \quad (1)$$

In this expression, A and the a_{km} are coefficients, $|\Omega\rangle$ is the vacuum state made of the full Fermi sea with an "empty" $4f$ orbital (no $4f$ electron in the case of Ce^{3+}, no $4f$ hole in the case of Yb^{3+}), with degeneracy N_f, $f_m^\dagger$ is the creation operator of a $4f$ state with magnetic quantum number m, and c_{km} is the annihilation operator of a conduction electron with quantum numbers k and m. The $4f$ states $|m\rangle$ are the eigenvectors, with energy ϵ_{fm}, of the crystal electric field interaction. The variational calculation of the energy E_0 of the ground N-electron state leads, in the case of a non-degenerate $4f$ shell, to the self-consistent equation, holding in the Kondo (or spin-fluctuation limit) [5,6]:

$$E_0 = -\frac{\Gamma}{\pi}\ln\prod_m \frac{D}{\epsilon_{fm} - E_0}, \quad (2)$$

where Γ is the bare hybridisation width and D the width of the conduction band. Introducing the single ion Kondo temperature T_K as the energy gain due to hybridisation ($T_K = \epsilon_{f1} - E_0$) and the crystal field splittings $\Delta_m = \epsilon_{fm} - \epsilon_{f1}$, equation (2) transforms into:

$$\prod_m (\Delta_m + T_K) = D^{N_f}\exp(-\frac{\pi\epsilon_f}{\Gamma}), \quad (3)$$

where $\epsilon_f \simeq \epsilon_{fm}$ is the energy of the $4f$ orbital below the Fermi level. The $4f$ "occupation numbers" at $T = 0$ are given by:

$$n_{fm} = \frac{\Gamma(1-n_f)}{\pi}\frac{1}{T_K + \Delta_m}\,. \quad (4)$$

where $n_f = \sum_m n_{fm}$ is the hole count in the $4f$ orbital, close to 1 in the Kondo limit of weak hybridisation. The parameters n_f, Γ and T_K are linked by the relationship, obtained by summing equation (4) over m:

$$\sum_m \frac{1}{T_K + \Delta_m} = \frac{\pi n_f}{\Gamma(1-n_f)}\,. \quad (5)$$

The mean value of an operator O acting on the $4f$ variables, in the ground state $|\psi\rangle$, *i.e.* at $T = 0$, can be written as [5]:

$$\langle O\rangle = \sum_m n_{fm}\langle m|O|m\rangle. \quad (6)$$

In the presence of an external magnetic field or of an exchange field H, the ionic splittings $\delta_m(H)$, eigenvalues of the crystal field Hamiltonian to which is added an electronic Zeeman interaction, and the field dependent Kondo temperature $T_K(H)$, defined as in zero field as the energy difference between the lowest ionic level and the Kondo singlet, are linked by an equation similar to equation (3). Then the following relationship holds:

$$\prod_m (T_K + \Delta_m) = \prod_m [T_K(H) + \delta_m(H)], \quad (7)$$

allowing to determine the renormalised Kondo temperature $T_K(H)$ as a function of the zero field value T_K. The occupation numbers in the presence of a field are then:

$$n_{fm}(H) = \frac{\Gamma(1-n_f)}{\pi}\frac{1}{T_K(H) + \delta_m(H)}\,. \quad (8)$$

The electronic observables in the presence of a magnetic field can then be derived as a function of the zero field Kondo temperature T_K by solving equation (7) for $T_K(H)$, and then using equations (6, 8).

A consequence of the presence of hybridisation, *i.e.* of a N-electron ground state containing a small admixture of the vacuum state $|\Omega\rangle$ with an empty $4f$ orbital, is that the $T = 0$ mean value of the observable O is modified with respect to its "hybridisation free" $T = 0$ value. For the spontaneous magnetic moment $m = -g_J J_z \mu_B$ (for Yb^{3+}: $g_J = 8/7$, $J = 7/2$), equation (6) always leads to a hybridised $T = 0$ moment smaller than the pure CEF moment, for a Kramers ion like Yb^{3+} or Ce^{3+}: this is the well-known magnetic moment reduction due to the Kondo screening. For the case of the $4f$ quadrupole moment $Q_{zz} = 3J_z^2 - J(J+1)$, the $T = 0$ (or saturated) value of $\langle Q_{zz}\rangle$ in the presence of hybridisation depends on the crystal field level scheme of the Yb^{3+} ion. In the case where the $4f$ quadrupole moment of the ground CEF state is large and positive, it will be shown in the next section that equation (6) leads to a reduction of the $T = 0$ $\langle Q_{zz}\rangle$ value with respect to the CEF value. These two quantities can be measured by ^{170}Yb Mössbauer spectroscopy: the spontaneous magnetic moment m is obtained in the magnetically ordered phase from the hyperfine field at the ^{170}Yb nucleus; and the principal component Q_{zz} of the quadrupole moment tensor is obtained in the paramagnetic phase from the electric field gradient at the nucleus. The Kondo reduction of both quantities arises from spin fluctuations, *i.e.* it is a dynamical effect at the rare earth site, and it is not due to the Kondo screening cloud of conduction electrons, which has an RKKY-like oscillatory behaviour in space [8]. So the moment values measured by Mössbauer spectroscopy at the nucleus site should be directly comparable with those calculated from the variational ground state $|\psi\rangle$.

3 The Mössbauer data and the variational calculation in the paramagnetic phase of the $YbCu_{5-x}Al_x$ series

The site symmetry of the Yb atom in the $YbCu_{5-x}Al_x$ series is very close to hexagonal (see for instance Ref. [7]). At 4.2 K and above, *i.e.* in the paramagnetic phase for all the compounds, the ^{170}Yb absorption Mössbauer spectrum is an axial quadrupolar hyperfine pattern, in agreement with

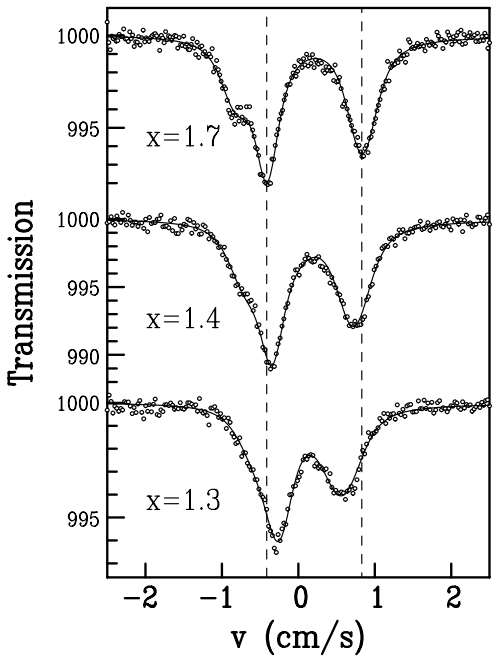

Fig. 1. ^{170}Yb Mössbauer absorption spectra at 4.2 K in $YbCu_{5-x}Al_x$ for $x = 1.7$ (top), 1.4 (middle) and 1.3 (bottom). The solid lines are fits to a Gaussian distribution of quadrupolar parameters. The dashed vertical lines mark the energies of the $\Delta m = \pm 1$ and $\Delta m = \pm 2$ transitions of the $x = 1.7$ spectrum. The corresponding splitting is worth $3\alpha_Q$, where α_Q is the quadrupolar hyperfine coupling parameter.

the hexagonal Yb site symmetry. The corresponding hyperfine Hamiltonian writes:

$$\mathcal{H}_Q = \alpha_Q \left[I_z^2 - \frac{I(I+1)}{3} \right], \qquad (9)$$

where $I = 2$ is the spin of the excited nuclear state of ^{170}Yb (the ground nuclear state has spin 0) and α_Q is the quadrupolar hyperfine coupling parameter. The measured quadrupolar hyperfine coupling parameter α_Q actually contains two contributions: the $4f$ part, proportional to $\langle Q_{zz} \rangle$, and a contribution from the lattice charges, which is difficult to estimate but whose order of magnitude amounts to 10-20% of the $4f$ contribution, with opposite sign:

$$\alpha_Q = B_Q \langle Q_{zz} \rangle + \alpha_Q^{latt}, \qquad (10)$$

with $B_Q = 0.276$ mm/s for ^{170}Yb.

Hyperfine quadrupolar spectra in the $YbCu_{5-x}Al_x$ series at 4.2 K for selected x values are shown in Figure 1. The spectra for all x values can be satisfactorily fitted using a rather narrow Gaussian distribution of α_Q values, with a mean square root deviation amounting to 10% of the central value, which originates from sample inhomogeneities. As can be seen in Figure 1, the overall quadrupolar splitting decreases as the Al content x decreases. The decrease of the fitted $T = 4.2$ K α_Q values as x decreases is shown in Figure 2. Using the reasonable assumption

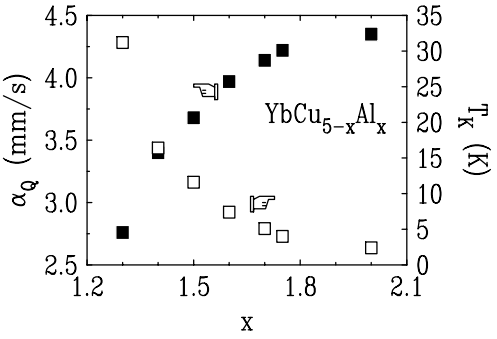

Fig. 2. Variation of the measured hyperfine quadrupolar coupling parameter α_Q (black squares) and of the derived single ion Kondo temperature (open squares) as a function of the Al content x in the $YbCu_{5-x}Al_x$ series.

that the lattice contribution α_Q^{latt} is constant throughout the $YbCu_{5-x}Al_x$ series, the decrease of α_Q with decreasing x is then due to a decrease of the $4f$ contribution, *i.e.* of $\langle Q_{zz}(T = 4.2\text{ K}) \rangle$. We will show here that this behaviour can be assigned to the increase of hybridisation as x decreases, and that it enables the values of the Kondo temperature T_K to be determined in the $YbCu_{5-x}Al_x$ series.

According to expression (6), the $T = 0$ value of the quadrupolar moment writes (the summation is over the 4 crystal field Kramers doublets, because two Kramers conjugate states have the same quadrupole moment):

$$\langle Q_{zz}(T=0) \rangle = \frac{2\Gamma(1-n_f)}{\pi} \sum_{i=1,4} \frac{\langle Q_{zz}^i \rangle}{T_K + \Delta_i}, \qquad (11)$$

where $\langle Q_{zz}^i \rangle$ is the $4f$ quadrupole moment of the ith state. The L_{III}-edge X-ray absorption data [1] have shown that the Yb valence, and thus the $4f$ hole count n_f, is constant throughout the series for $x \geq 1.3$, with $n_f \simeq 0.98$. As to the crystal field energies Δ_i, a recent study of the resistivity in the $YbCu_{5-x}Al_x$ series [9] indicates that there is no drastic change of the crystal field splittings as the Al content varies. We can therefore adopt as a reasonable assumption that the CEF interaction is constant throughout the series. Then $\langle Q_{zz}(T = 0) \rangle$ is a function of T_K only through equations (11, 5), and it is easy to show that the leading term of the derivative $\frac{d\langle Q_{zz} \rangle}{dT_K}$ is proportional to $Q_{zz}^2 - Q_{zz}^1$. Therefore the behaviour of $\langle Q_{zz} \rangle$ as a function of T_K depends on the difference of the $4f$ quadrupole moments of the first excited CEF state and of the ground state. According to reference [7], the Yb^{3+} ground state ($\Delta_1 = 0$) of the hexagonal crystal field interaction in $YbCu_3Al_2$ is:

$$|\phi_g\rangle = 0.99 \left| \pm \frac{7}{2} \right\rangle \pm 0.14 \left| \mp \frac{5}{2} \right\rangle, \qquad (12)$$

the first CEF excited state contains the same basis vectors as $|\phi_g\rangle$, but is orthogonal to it, and lies at $\Delta_2 \simeq 100$ K, and the two other doublets lie at energies higher than 150 K above the ground state. Then: $Q_{zz}^1 = 20.64$ and

Table 1. Values of the quadrupolar hyperfine coupling parameter α_Q, the Kondo and magnetic transition temperatures, the saturated spontaneous magnetic moment, the exchange constant and the exchange energy in the $YbCu_{5-x}Al_x$ series. The origin of the discrepancy between the spontaneous $T = 0$ moment values derived from ^{170}Yb Mössbauer spectroscopy and neutron diffraction is still an open question.

x	1.3	1.4	1.5	1.6	1.7	1.75	2
α_Q (mm/s)	2.75	3.40	3.70	4.00	4.15	4.20	4.35
T_K (K)	31.2	16.4	11.6	7.4	5.1	4.0	2.4
T_N (K)				0.25	0.55	1.0	2.0
$m(T=0)$ (μ_B)[a]				0.1	0.7	2.0	2.85
$m(T=0)$ (μ_B)[b]						1.2	2.1
λ (kOe/μ_B)				8.3	5.7	5.0	3.7
E_{ex} (K)				8.3	5.7	5.0	3.7

[a]Saturated spontaneous moment values obtained by ^{170}Yb Mössbauer spectroscopy in the present work.
[b]Saturated spontaneous moment values obtained from the neutron diffraction data assuming an antiferromagnetic structure with propagation vector $\mathbf{k} = (1/2, 1/2, 0)$ and the moments parallel to the **c** axis [1].

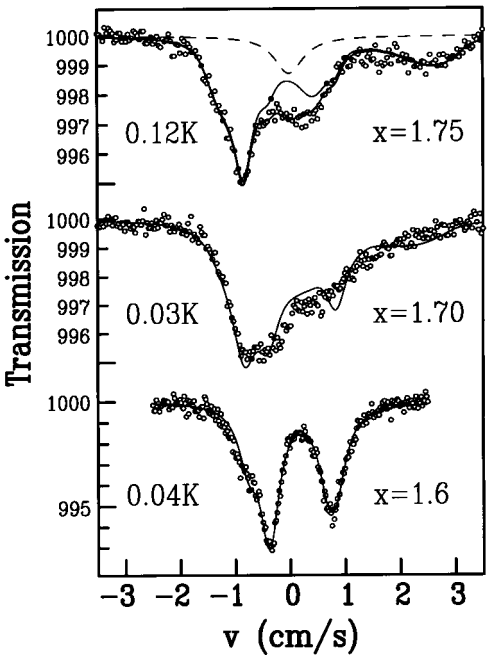

Fig. 3. ^{170}Yb Mössbauer absorption spectra in $YbCu_{3.25}Al_{1.75}$ at 0.12 K (top), in $YbCu_{3.3}Al_{1.7}$ at 0.03 K (middle) and in $YbCu_{3.4}Al_{1.6}$ (bottom). The dashed line in the $x = 1.75$ spectrum represents an impurity phase containing non-magnetic Yb ions (probably $YbCu_4Al$). The solid lines are fits using the variational calculation, as explained in Section 5, for $x = 1.75$ and 1.7, and using a standard hyperfine line shape for $x = 1.6$.

$Q_{zz}^2 = 3.36$, and the $T = 0$ hybridised value $\langle Q_{zz} \rangle$ is a decreasing function of T_K ($\frac{d\langle Q_{zz}\rangle}{dT_K} < 0$). Furthermore, as $\Delta_2 \simeq 100$ K, the $T = 4.2$ K values of the quadrupolar moment can be considered as the saturated $T = 0$ values. We therefore interpret the experimentally observed decrease of $\alpha_Q(T = 4.2\text{ K})$ as x decreases in the $YbCu_{5-x}Al_x$ series as due to the increase of the Kondo temperature.

In order to make a more quantitative analysis, we must assess a complete CEF level scheme for the Yb^{3+} ion at its site with hexagonal symmetry. We will model the CEF interaction in the $YbCu_{5-x}Al_x$ series according to the above considerations for the two first excited states, and assume the two remaining states lie at 300 K and 400 K above the ground state. The choice of these two latter energies is rather arbitrary, but their influence on the final result is small. The hexagonal CEF interaction can be expressed in terms of the operator-equivalents O_n^m [10]:

$$\mathcal{H}_{hex} = B_2^0 O_2^0 + B_4^0 O_4^0 + B_6^0 O_6^0 + B_6^4 O_6^4. \qquad (13)$$

The assumed CEF level scheme for Yb^{3+} corresponds to: $B_2^0 = -10.27$ K, $B_4^0 = 1.3 \times 10^{-2}$ K, $B_6^0 = 9.7 \times 10^{-3}$ K and $B_6^4 = 1.47 \times 10^{-2}$ K.

For the less hybridised alloy of the series, $YbCu_3Al_2$, the Kondo temperature was estimated to be around 2.5 K [7]. We choose here: $T_K = 2.4$ K in this compound, which allows to obtain the $\langle Q_{zz} \rangle$ value at $T = 0$ from equation (11) and then the lattice contribution α_Q^{latt} by comparison with the experimental α_Q value according to equation (10). One obtains: $\alpha_Q^{latt} \simeq -1$ mm/s, which is a correct order of magnitude. Using the assumption that α_Q^{latt} is constant throughout the series, one gets the Kondo temperature for the other members of the $YbCu_{5-x}Al_x$ series from the measured α_Q values using equation (11). The T_K values are represented in Figure 2 (see also Tab. 1); they increase first moderately as x decreases, then show a rapid upturn for $x \leq 1.5$. Such a variation is expected in the frame of the variational approach, where the Kondo temperature can be shown to grow exponentially as hybridisation increases. For another choice of T_K in $YbCu_3Al_2$ around 2.5 K, the value of α_Q^{latt} would be slightly different, resulting in a small shift of the Kondo temperature values, but with no effect on the main trend of variation of T_K with x.

4 The magnetically ordered phase in the $YbCu_{5-x}Al_x$ series

The compound $YbCu_3Al_2$ shows antiferromagnetic ordering of the Yb^{3+} moments [11,7] with $T_N = 2$ K and a saturated magnetic moment of 2.85 μ_B. As x decreases, the increasing hybridisation reinforces the Kondo screening of the Yb^{3+} moment and both the magnetic transition temperature and the saturated moment are expected to decrease [12]. We present here Mössbauer data for the three compounds with $x = 1.75$, 1.7 and 1.6, and magnetic susceptibility curves for $x = 1.7$ and 1.6.

4.1 $YbCu_{3.25}Al_{1.75}$ and $YbCu_{3.3}Al_{1.7}$

The compound with $x = 1.75$ shows a peak of the specific heat at 1 K [1] which is attributed to the onset of magnetic ordering. The Mössbauer spectrum at 0.12 K, represented at the top of Figure 3, can be fitted using a standard axial

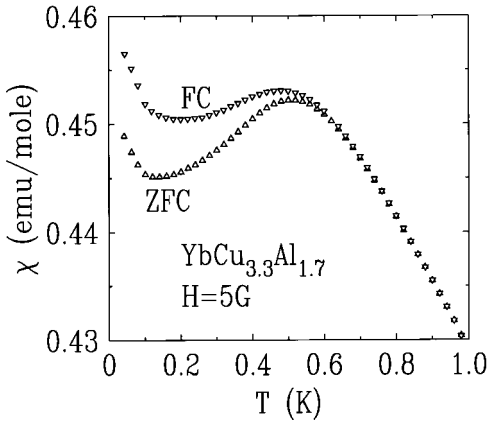

Fig. 4. Magnetic susceptibility curves in $YbCu_{3.3}Al_{1.7}$ with a field of 5 G. The FC and ZFC curves deviate from each other below the irreversibility point at 0.55 K.

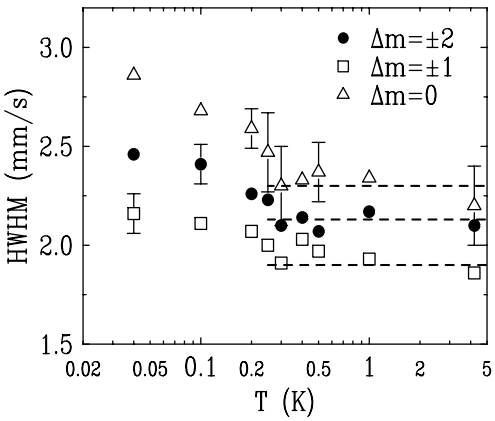

Fig. 5. Thermal variation of the half width at half maximum (HWHM) of the three Lorentzian-shaped lines of the quadrupolar hyperfine spectrum in $YbCu_{3.4}Al_{1.6}$. The dashed lines are guides for the eye and represent the mean constant values of the HWHM between 0.25 K and 5 K.

magnetic hyperfine line shape where the line positions are the eigenvalues of the hyperfine Hamiltonian:

$$\mathcal{H}_{hf} = -g_n\mu_n I_z H_{hf} + \mathcal{H}_Q, \tag{14}$$

where $g_n\mu_n I$ is the magnetic moment of the excited nuclear state and H_{hf} the hyperfine field at the ^{170}Yb nucleus. One must allow for different (inhomogeneous) line widths, which will be shown in Section 5 to be well accounted for by crystal field inhomogeneities. A good fit (identical with that represented by the solid line in Fig. 3 top) is obtained with a mean hyperfine field of 2000 kOe at the ^{170}Yb nucleus. The saturated spontaneous Yb^{3+} moment for $x = 1.75$ is therefore $m \simeq 2\,\mu_B$, using the hyperfine constant for $^{170}Yb^{3+}$ of 1020 kOe per μ_B. This value is reduced with respect to that in $YbCu_3Al_2$ ($2.85\,\mu_B$) due to the increased Kondo screening.

In $YbCu_{3.3}Al_{1.7}$, the Mössbauer spectra are quadrupolar hyperfine spectra down to 0.6 K, with however spectral distortions due to electronic fluctuations in the frequency range 500 MHz – 1 GHz. Below 0.4 K, the spectra change shape and can be interpreted in terms of the static magnetic hyperfine interaction (14). The spectrum at 0.03 K, shown in the middle of Figure 3, clearly has a reduced hyperfine splitting with respect to that in $YbCu_{3.25}Al_{1.75}$. Reproducing the details of the experimental spectral shape with a standard hyperfine line shape (fit similar to that represented by the solid line in Fig. 3 middle) is rather difficult due to a pronounced inhomogeneity of the linewidths. However, the hyperfine field can be determined rather accurately from the negative velocity part of the spectrum, where the lines are narrower (see also the spectrum for $x = 1.75$). We obtain a mean hyperfine field of $\sim$ 700 kOe, corresponding to a spontaneous Yb^{3+} moment of $\sim 0.7\,\mu_B$. It will be shown in Section 5 that the line broadenings for $x = 1.7$ cannot be entirely reproduced by crystal field inhomogeneities alone, suggesting the presence of another parameter distribution, probably of exchange fields. In order to determine the magnetic transition temperature in this compound more accurately, we performed magnetic susceptibility measurements in a home-made ^{3}He–^{4}He dilution refrigerator with a SQUID magnetometer, with a field of 5 G, and using both zero-field cooling (ZFC) and field cooling (FC) procedures. The low temperature part of the magnetic susceptibility curve $\chi(T)$ in $YbCu_{3.3}Al_{1.7}$ is shown in Figure 4. The transition to a magnetically ordered phase is seen to occur around 0.5 K, in good agreement with the Mössbauer data. The ZFC and FC curves are distinct below 0.55 K, indicating the presence of irreversibilities in the magnetic behaviour. The latter could be induced by disorder or frustration in the Yb-Yb interactions, leading to a distribution of exchange fields as suggested above, and to a spin-glass like ordering. Below 0.1 K, an upturn is visible on both curves, which could originate from Yb ions experiencing a vanishingly small exchange field and thus behaving as paramagnetic ions.

4.2 $YbCu_{3.4}Al_{1.6}$

The Mössbauer spectra in this compound are quadrupolar hyperfine spectra down to the lowest temperature (see the spectrum at 0.04 K at the bottom of Fig. 3). However, the individual linewidths corresponding to the three nuclear transitions with $\Delta m_I = 0, \pm1, \pm2$ reveal a sizeable increase as temperature is lowered below 0.25 K (see Fig. 5). The lines of a quadrupolar hyperfine spectrum can be broadened by a distribution of electric field gradients, or by the presence of a small hyperfine field which splits or mixes the quadrupolar transitions. As a change in the electric field gradients can be safely ruled out at such a low temperature, we can conclude that the observed broadenings are due to the presence of a small hyperfine field, reaching 100 kOe at 0.04 K. Therefore, the compound $YbCu_{3.4}Al_{1.6}$ shows the onset of a magnetically ordered phase below 0.25 K, with a very small saturated Yb^{3+} moment of $\simeq 0.1\,\mu_B$. The low temperature magnetic

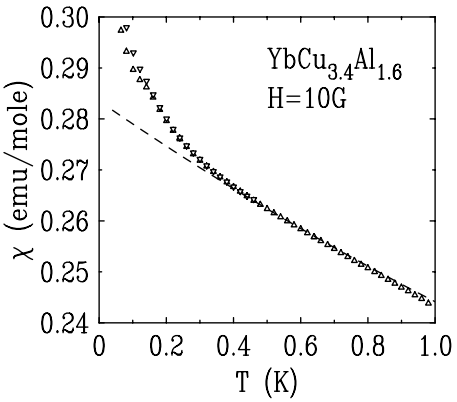

Fig. 6. Magnetic susceptibility curves in $YbCu_{3.4}Al_{1.6}$ with a field of 10 G. The FC (∇) and ZFC ($\triangle$) curves are almost indistinguishable and slightly deviate from each other below 0.15 K. The dashed line is a Curie-Weiss law obeyed in the temperature range from 0.4 K to 4.2 K.

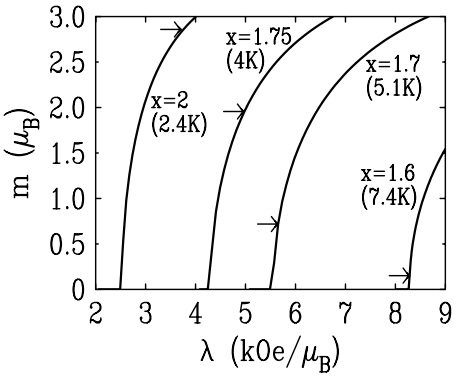

Fig. 7. Variation of the $T = 0$ spontaneous magnetic moment of the Yb^{3+} ion as a function of the molecular field constant λ for Kondo temperature values corresponding to those obtained in the $YbCu_{5-x}Al_x$ series: $T_K = 2.4$, 4, 5.1 and 7.4 K for $x =$ 2, 1.75, 1.7 and 1.6. The arrow on each curve indicates the experimental value of the spontaneous Yb^{3+} moment.

susceptibility, measured in a field of 10 G, is shown in Figure 6. One observes a deviation from a paramagnetic Curie-Weiss law (dashed line in Fig. 6) below $\simeq$ 0.3 K. This anomaly (at 0.3 K) is different from that occurring (at 0.55 K) in $YbCu_{3.3}Al_{1.7}$: it is rather ferromagnetic-like, and furthermore the FC and ZFC curves are practically identical. The temperature at which the susceptibility anomaly occurs is close to that where the Mössbauer linewidths anomaly occurs, and marks the transition to the magnetically ordered state. The alloy $YbCu_{3.6}Al_{1.6}$ lies therefore very close to the magnetic instability; for a slightly smaller Al content, *i.e.* for $x = 1.5$, no anomaly in the Mössbauer line broadenings is observed down to 0.06 K. The alloy $YbCu_{3.5}Al_{1.5}$ thus does not show magnetic ordering down to this temperature. For these two alloys very close to the magnetic instability, a clear Non-Fermi liquid behaviour has been evidenced in [9] by the specific heat data.

5 The variational calculation in the magnetically ordered phase of the $YbCu_{5-x}Al_x$ series

The variational approach is applied here to the calculation of the $T = 0$ spontaneous magnetic moment for $1.6 \leq x \leq 2$. We used a mean field approximation by introducing an exchange field $\mathbf{H}_{ex} = \lambda \mathbf{m}$, where λ is a molecular field constant reflecting the strength of the RKKY interionic interaction; it is taken to be positive in order to describe a local exchange field due to a collinear magnetic structure. The Hamiltonian of the problem is now the hexagonal CEF interaction (13) to which is added the exchange interaction. Using a self-consistent calculation, we computed the $T = 0$ spontaneous moment as a function of the molecular field constant λ, for different values of the zero field Kondo temperature T_K, using equation (7) and expression (6) where $O = -g_J \mu_B J_z$ (we assume the spontaneous moment lies along the hexagonal **c** axis, as was demonstrated for $x = 2$ and 1.75 by neutron diffraction measurements [1]). The results are shown in Figure 7, where the $m = f(\lambda)$ curves were calculated for the T_K values obtained for $x = 2$, 1.75, 1.7 and 1.6. For each value of the Kondo temperature, there is a critical λ value below which no spontaneous moment exists, *i.e.* below which the Kondo spin fluctuations overcome the exchange interaction. Above this critical λ value, the $T = 0$ spontaneous moment steadily grows as λ increases, eventually reaching a value close to the hybridisation free saturated value $m_0 = g_J \mu_B \langle \psi_g | J_z | \psi_g \rangle = 3.86\, \mu_B$. The molecular field constant obtained for each value of x can be read off in Figure 7 (see Tab. 1), the experimental spontaneous moment values being indicated by an arrow on each curve. The λ value obtained herewith for $x = 2$ (3.7 kOe/μ_B) is in good agreement with that derived in reference [7] from a fit of the $T = 1.5$ K magnetisation (3.5 kOe/μ_B). The RKKY exchange energy scale can be defined as: $E_{ex} = \lambda m_0^2$, and its values in the $YbCu_{5-x}Al_x$ series are given in Table 1. The noticeable feature here lies in the fact that the molecular field constant (and thus the exchange energy) values increase as x decreases, *i.e.* as hybridisation increases. The hybridisation strength is reflected in the value of the dimensionless parameter $g = \Gamma/|\epsilon_f|$. The RKKY energy scale T_{ex} varies as g^2 whereas the Kondo energy scale varies as $\exp(-1/g)$, as first pointed out by Doniach [12]. When the two interactions are present as in the $YbCu_{5-x}Al_x$ series, they compete with respect to the establishment of magnetic ordering. So as hybridisation increases, it is expected that both energy scales increase and that the temperature T_N of the magnetic transition (as well as the spontaneous magnetic moment) decreases, up to a critical point where T_N vanishes [12]. So in Kondo lattices close to this critical point of the magnetic instability, the transition temperature can be much smaller than the exchange energy [13]. In the present $YbCu_{5-x}Al_x$ series, the general trend of variation of the two derived energy scales T_{ex} and T_K, as well as that of the magnetic

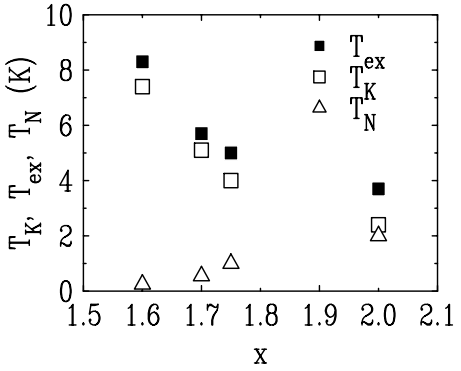

Fig. 8. Variation of the Kondo temperature, of the exchange energy and of the magnetic transition temperature as a function of the Al content x in the $YbCu_{5-x}Al_x$ series.

transition temperature T_N, with the Al content x agree well with Doniach's phase diagram, as seen in Figure 8.

The fits of the Mössbauer spectra from which were obtained the magnetic moment values in Section 4 were phenomenelogical fits using the hyperfine Hamiltonian (14), and the line widths were taken as adjustable parameters. Here, we use the above described variational calculation to compute the $T = 0$ Mössbauer spectra in the magnetically ordered compounds. In this *ab initio* calculation, the input parameters are the crystal field parameters, the Kondo temperature and the molecular field constant, with values as determined previously. The exchange field is treated in a self consistent way, and is assumed to be parallel to the hexagonal **c** axis. In order to reproduce the inhomogeneous broadenings of the lines, it was necessary to allow for a distribution of distortions from the nominal hexagonal site symmetry. A Gaussian distribution of the B_2^0 CEF parameter was introduced; the resulting line shapes (solid lines in Fig. 3) agree very well with the experimental spectra with a root mean square deviation $\sigma(B_2^0) = 0.35$ K, amounting to 3.5% of the central B_2^0 value (-10.27 K), for $x = 2$ (not shown, but similar to the fit for $x = 1.75$) and 1.75. For $x = 1.70$, the overall hyperfine splitting is correctly reproduced, but the line broadenings could not be satisfactorily accounted for. This suggests, as already pointed out in Section 4, that an additional broadening mechanism is at play, probably a distribution of exchange fields, and that the magnetic structure is more complicated that simply collinear antiferromagnetic and could be of spin-glass type. For $x = 1.6$, where the magnetic moment is very small, the variational procedure does not yield good results, and the corresponding solid line in Figure 3 for $x = 1.6$ is a fit with a standard hyperfine field line shape. The inadequacy of the variational calculation for this Al content could also be due to an unconventional type of magnetic structure.

6 Conclusion

The variational solution of the impurity Kondo problem has been used to interpret the very low temperature properties of the Yb^{3+} ion in the Kondo lattices $YbCu_{5-x}Al_x$, when the Al content x varies from 1.3 to 2. The single ion Kondo temperatures in this series have been deduced from the $T = 0$ values of the $4f$ quadrupole moment measured by ^{170}Yb Mössbauer spectroscopy. Just above the critical value $x_c = 1.5$ below which the compounds do not show magnetic ordering, we have detected a magnetic transition at $T = 0.25$ K for $x = 1.6$ and at 0.55 K for $x = 1.70$. The values of the magnetic transition temperatures obtained by Mössbauer spectroscopy and by magnetic measurements are in very good agreement. A self-consistent mean field calculation in the frame of the variational approach was used in order to determine the exchange energy from the $T = 0$ spontaneous moment value for $1.6 \leq x \leq 2$. We find that both the Kondo temperature and the exchange energy increase as the $4f$-conduction electron hybridisation becomes stronger, *i.e.* as x decreases, whereas the temperature of the magnetic transition decreases and eventually vanishes for $x < 1.6$. This behaviour is in good general agreement with the predictions of Doniach's model describing the competition between the Kondo coupling and the exchange interaction for the establishment of magnetic ordering in Kondo lattices.

We wish to thank P. Pari and M. Ocio, from the "Service de Physique de l'État Condensé", who designed the dilution refrigerators used in this work for the Mössbauer and SQUID measurements.

References

1. E. Bauer, R. Hauser, L. Keller, P. Fischer, O. Trovarelli, J.G. Sereni, J.J. Rieger, G.R. Stewart, Phys. Rev. B **56**, 711 (1997).
2. P. Fulde, J. Keller, G. Zwicknagl, Solid State Phys. **41**, 1 (1988).
3. O. Gunnarsson, K. Schönhammer, Phys. Rev. B **28**, 4315 (1983).
4. K. Hanzawa, K. Yamada, K. Yosida, J. Magn. Mat. **47-48**, 357 (1985).
5. G. Le Bras, Ph.D. thesis, University of Orsay, France (1994) unpublished
6. L.C. Andreani, E. Liviotti, P. Santini, G. Amoretti, Z. Phys. B **100**, 95 (1996).
7. P. Bonville, E. Bauer, J. Phys.-Cond **8**, 7797 (1996).
8. E. Pavarini, L.C. Andreani, G. Amoretti, Physica B **206-207**, 144 (1995).
9. E. Bauer, R. Hauser, A. Galatanu, G. Hilscher, H. Michor, J. Sereni, M.G. Berisso, P. Pedrazzini, M. Galli, F. Marabelli, P. Bonville, submitted to Phys. Rev. B.
10. A. Abragam, B. Bleaney, *Electron paramagnetic resonance of transition ions* (Clarendon Press, Oxford, 1970).
11. E. Bauer, E. Gratz, L. Keller, P. Fischer, A. Furrer, Physica B **186-188**, 608 (1993).
12. S. Doniach, Physica B **91**, 231 (1977).
13. P. Bonville, J.A. Hodges, F. Hulliger, P. Imbert, G. Jéhanno, J.B. Marimon da Cunha, H.R. Ott, Hyperfine Interact. **40**, 381 (1988).